Biblid: 1450-5029, (2024) 28; 1; p 31 - 37
UDK: 629.762
DOI: 10.5937/jpea28-49495
Original Scientific Paper

APPLICATION OF FLOW VISUALIZATION METHODS FOR DETERMINING DRAG FORCE AROUND A PROJECTILE

PRIMENA TEHNIKA VIZUELIZACIJE STRUJANJA ZA ODREĐIVANJE SILE OTPORA PROJEKTILA

Vladimir KOZOMORA[1], Andreja ŽIVKOV[1], Marko VUKIĆ[1], Nikola OLUŠKI[1]
[1]University of Novi Sad, Faculty of Technical Sciences, Novi Sad, Trg Dositeja Obradovića 6, Serbia
**Correspondence: andreja.zivkov@uns.ac.r*

ABSTRACT

The paper provides an overview of flow visualization methods. From the many ways of classifying flow visualization methods, the chosen method of classification is in accordance with the experimental procedure. Flow visualization methods that involve the addition of foreign material are the simplest, from the point of view of the required material and the experimental setup, in which one tracer and an adequate light source are most often applied, except for layers sensitive to pressure and shear stress. Their application is wide and most methods from this category can be modified very easily depending on the case. Visualization methods that involve addition of energy to the fluid flow use strong sources of electromagnetic radiation, most often lasers, to excite the molecules in the fluid stream, producing an adequate quantum-mechanical effect that enables visualization. Optical methods of flow visualization are based on changes in the refractive index of light caused by the presence of a fluid in motion in the test section, in addition, the principle of superposition of light waves is used in interferometry methods. Optical methods are mainly used in areas of supersonic flow and shock wave studies, but they are also present in exhaust gas propagation studies. As computational fluid dynamics is a separate subject, the physical laws on which CFD is based on are presented, as well as an example of flow visualization, which is an integral part of most calculations performed using this method. In addition to the classification and description of flow visualization methods, the paper provides an explanation of a approximate calculation procedure based on the use of one of the optical methods, Schlieren photography, in order to calculate the resistance force during supersonic projectile flow, as well as a comparison of results based on empirical data.

Keywords: *visualization, Schlieren photography*

REZIME

U radu je dat pregled metoda vizuelizacija strujanja. Od mnogobrojnih načina podela metoda vizuelizacije strujanja odabrana je metodologija podele u skladu sa eksperimentalnim postupkom. Metode vizuelizacije strujanja koje podrazumevaju dodavanje stranog materijala su najjednostavnije, sa stanovišta potrebnog materijala i postavke eksperimenta, u okviru kojih se najčešće primenjuje jedan „trejser" i adekvatan izvor svetlosti, izuzev slojeva osetljivih na pritisak i smicanje. Kakateristične metode ove grupe se baziraju na principu eletrolize i elektrolitičke percipitacije ili jednostavnim bojama, ali to mogu biti i metode koje koriste pločice guanuina ili neki specijalizovan trejser.. Njihova primena je široka i većina metoda se može vrlo lako modifikovati u zavisnosti od slučaja koji je potrebno sagledati. Metode vizuelizacije koje podrazumevaju dodavanje energije fluidnoj struji koriste jake izvore elektromagnetnog zračenja, najčešće lasera, zarad pobude molekula koji se nalaze u fluidnoj struji proizvodeći adekvatan kvantno-mehanički efekat koji omogućava vizuelizaciju. Metode ove grupe se baziraju na pobudi elektrona fotonima i njihovoj reklasaciji kojom se emituje svetlost. Ove metode se najčešće koriste za izučavanja procesa sagorevanja, graničnog sloja i kompleksne strujne slike. Optičke metode vizuelizacije strujanja se baziraju na promenama indeksa prelamanja svetlosti koje su prouzrokovane prisustvom fluida u pokretu u ispitnoj sekciji, pored toga se koristi i princip superpozicije svetlosnih talasa u metodama interferometrije. Optičke metode su uglavnom najviše primenjivane u oblastima izučavanja nadzvučnog strujanja i udarnih talasa, ali su prisutne i pri propagacijama izduvnih gasova. Kako je računarska dinamika fluida sama za sebe zasebna oblast predstavljeni su fizički zakoni na osnovu kojih je RDF bazirana, kao i primeri vizuelizacije strujanja, koja je sastavni deo u većini proračuna izvedenih ovom metodom. Pored klasifikacije i opisa metoda vizuelizacije strujanja u radu je dato objašnjenje postupka aproksimativnog proračuna na osnovu upotrebe jedne od optičkih metoda, šliren fotografije, u cilju izračunavanja sile otpora prilikom supersoničnog strujanja projektila kao i poređenje rezultata proračunom baziranom na osnovu empirijskih podataka.

Ključne reči*: vizuelizacija, šliren fotografija*

INTRODUCTION

The study of fluid flows and various phenomena related to them has been the subject of many researchers for centuries. Flow visualization methods date back to the period when Leonardo da Vinci observed vortex phenomena and drew them. In modern times flow visualization methods are paired with technological advancements such as high speed cameras, advanced picture processing methods, etc. Some of the areas where the experimental visualization of flow has contributed the most are the visualization of various phenomena in earlier periods of flow study, the transition of flow regimes, vortex dynamics, heat transfer in fluids, the study of boundary layers, in medicine where the study of blood flow has led to better diagnostics and treatment of cardiovascular diseases and in the field of environmental protection which enables having an insight into dispersion of poluttants eg., as well as an educational tool. Naturally, flow visualization methods are also present in engineering practices. The flow of compressible fluids is important for the development of automobiles, airplanes, spacecraft, as well as for the construction of machines such as turbines and internal combustion engines. On the other hand, the flow of incompressible fluids is important in maritime engineering for the construction of ships and various elements

such as arches and protective costal elements. A similar publication is AJ Smiths & TT Lim Flow Vizualisation that uniquely among similar publications focuses on the practical rather than theoretical aspects as well as obtaining high quality flow visualization for the purpose of obtaining a complete understanding of the flow behavior. Another one is Wolfgang Merzkirch Flow Vizualisation which focuses on developments, applications, and results in the field of flow visualization, and presents it in the form of surveys of available tracer materials, techniques of introducing the tracer to the flow, techniques of proper illumination of the flow scene etc. The purpose of this paper is to give an overview of the most used flow vizualisation methods and to analize their different applications.

Nomenclature:

p – pressure [Pa]
F_D – drag force [N]
M – Mach number [-]
P – surface [m^2]
R – specific gas constant [J/kgK]
T – temperature [K]
c – velocity of sound [m/s]
h – altitude [m]

Greek letters:

α – attack angle [°]
β – shock wave angle [°]
θ – deflection angle [°]
μ – kinematic viscosity [m^2/s]
λ – thermal conductivity [W/mK]

List of indexes:

1 – value before shock wave
2 – value after shock wave
a – perpendicular projection to the shock wave
D – based on θ-β-M diagram
S – based on Schlieren photograph

List of acronyms:

CFD – Computational fluid dynamics
CCD – Charge-coupled device

THEORETICAL MODEL

Until recently, experimental flow visualization was the primary method for examining fluid flows, but today with the increase in computational power, computational fluid dynamics also contributed to flow visualization methods. The purpose of experimental flow visualization is multifaceted. It was developed with the aim of understanding the fluid flow around a model as precisely as possible, without the need for calculations. As well as creating and validating new and existing models, which is now crucial in the field of CFD. Flow visualization methods can be divided into large groups based on the principle in use that can be further subdivided by specific characteristics:

1) Adding extraneous material:
   - Hydrogen bubble visualization,
   - Smoke and paint visualization,
   - Tuft visualization,
2) Adding energy:
   - Molecular tagging,
3) Optical methods:
   - Schlieren method,
   - Digital interferometry.
4) Computational fluid dynamics.

Flow visualization by using hydrogen bubbles is based on the creating a lot small hydrogen bubbles in the process of electrolysis. Hydrogen bubbles are created on a very thin conductive wire (25-50 μm), which acts as one of the electrodes in the direct current circuit, while the other electrode is usually a metal or graphite material that is placed outside the test zone but in the fluid flow. The direction of the current should be established so that the wire is the negative electrode in order to form hydrogen bubbles on its surface. Oscillating the voltage through the wire creates successive lines of hydrogen bubbles separated by constant time intervals. These bubble lines are called timelines. The bubble line formed on the wire is carried downstream by the fluid current and deforms according to the local velocity profile. The diameter of the hydrogen bubbles is 1-1.5 times larger than the diameter of the wire so that the speed of the bubbles rising due to the Stokes law has a negligible influence in relation to the local speed of the fluid flow. The very shape and orientation of the wire will depend on the type of fluid flow that is examined. In addition, an important parameter is the distance of the wire supports, which are subject to vortex shedding, which will disrupt the flow being tested. For the material of the wire stainless steel, aluminum, tungsten and platinum is used. Platinum is most commonly used material since it is noncorrosive and has good soldering properties. If the formed bubbles are adequately illuminated, a detailed visualization of the flow is possible, and together with photographs, quantitative analysis are also possible. For illumination, a background light is used that is tilted relative to the plane of bubble formation, whose angle is determined by trial and error but the recommended angle is 65º *(Frits, H. and Walsum, T. 1993; Quraishi, M. and. Fahidy, T. 1986; Merzkirch, W. 1987).*

One of the oldest methods of visualization of the movement of fluids in motion is the use of dye and smoke. Dyes, which are most commonly food dyes, are also the simplest method. To reduce the buoyancy of the dye, it is mixed with small amounts of alcohol, methanol or ethanol. In addition to food coloring, laundry detergent, milk, fluorescent dye, potassium permanganate and rhodamine are also used. Essentially any substance having neutral buoyancy, resistance to mixing with the fluid being tested, and good visibility can be used. The dye is usually injected into the fluid stream using a small diameter pipe (1.5-2 mm) or in some cases along with the help hypodermic needles or openings on the model through which the dye can be injected, Figure 1.

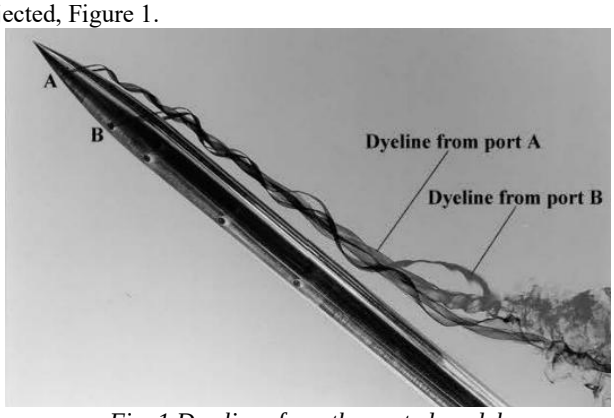

Fig. 1 Dye lines from the ported model

However, in this way of administering the dye its velocity injection can disrupt the fluid flow, which is being examined, too high velocity will produce mushroom like disruptions. On the other hand, too low velocity produces a vortex street. In both cases the disruptions will affect the fluid flow and result in inaccurate visualization. These disturbances can be reduced by placing the dye source further upstream. *(Frits, H. and Walsum, T. 1993; Quraishi, M. and. Fahidy, T. 1986; Smiths, A.J.and Lim, T.T. 2012).*

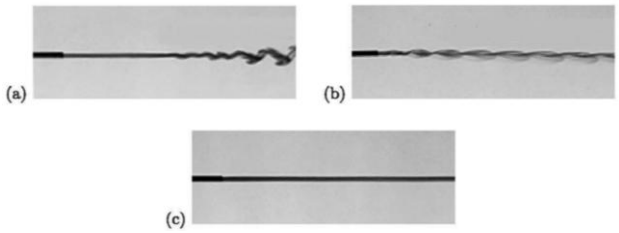

Fig. 2 Influence of dye injection velocity a) too high; b) too small; c) adequate (Smiths, A.J.and Lim, T.T. 2012)

A smoke wire is one of the most common methods for visualizing airflow. A wire with some hydrocarbon oil on it, which is then heated by passing current resulting in oil evaporation. The wire is metal, the type of material is not important as long as it meets the requirements in terms of tensile strength and electrical resistance. The most commonly used materials are nickel, steel and tungsten. The diameter of the wire depends on the velocity of the fluid flow, smaller diameters corresponding to smaller velocity values and vice versa. It is important that the wire is evenly covered in oil. The oil can be applied manually or automatically using brushes. (*Merzkirch, W. 2007; Quraishi, M. and. Fahidy, T. 1986; Smiths, A.J.and Lim, T.T. 2012; Merzkirch, W. 1987).*

Using tufts is a simple way to get an idea of the flow direction near the solid surface to which the tufts are attached. If the flow becomes unstable in the transition regime or completely turbulent, the tufts start to move very restlessly, which can be an indication that the boundary layer has become turbulent. An even more chaotic movement of the tufts can be an indication that it came from the separation of the boundary layer. The choice of tuft size and material depends on the size of the model being tested and the conditions under which it will be tested. For example, ordinary cotton threads several centimeters long are used for testing on cars or airplanes, but their size as well as the glue used to fix them to the surface significantly influences the air flow on the surface. Mini tufts have been developed to reduce the negative influence on the fluid flow, they are made from thin nylon strands with the overall diameter around 20 μm. They can also be treated with fluorescent color for increased visibility, Figure 3. The tips themselves tend to develop a very high frequency whiplash motion which makes them difficult to photograph. In such cases, small cups are connected to the free end of the tufts, which are narrow, solid and usually hollow in order to reduce their mass and to calm the movement of the tufts (*Frits, H. and Walsum, T. 1993; Quraishi, M. and. Fahidy, T. 1986; Merzkirch, W. 1987).*

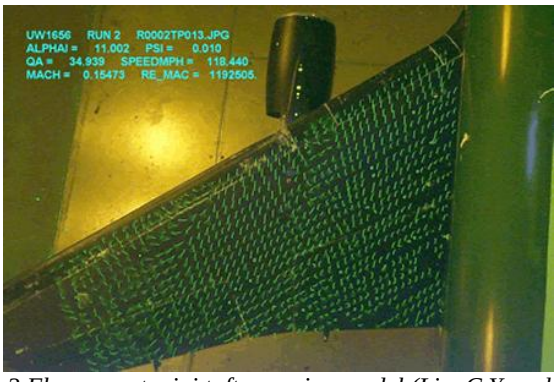

Fig. 3 Fluorescent mini tufts on wing model (Liu, C.Y. and Ng, K.L. 1990)

Molecular tagging is a method that involves the use of lasers and molecules as tracers. When the tracers are excited by a laser, they become marked for a longer period of time and are carried by the fluid flow. After a certain interval, the tagged molecules are photographed with a special camera such as a CCD (charged-coupled device) or some other camera to obtain an image of the traveled distance of the marked molecules. The tracers used can be a photochromic dye or phosphorescent supramolecules. Photochromic tracers are initially transparent in the visible spectrum, and upon absorption of a single photon, they begin to absorb light in a wider spectrum. Then when illuminated by white light, the fluid containing this photochromic color appears to be dark in color, while the dye is visible. In addition to the photochromic dye, fluorescein can be used, which has a high quantum yield that describes how many times a specific event will occur per one absorbed photon and is approximatelly 85%. This method is then called laser-induced fluorescence. Photochromic ink is relatively inexpensive and the marking process can be performed with a nitrogen gas laser. The methods using these tracers are extremely suitable for studying the mixing of two fluid streams because the mixing zones themselves are very clearly visible. Ozone can be used to visualize the gas phase. The use of ozone for visualization is based on the selective absorption of ultraviolet light by ozone. In the visible light spectrum, ozone is completely transparent while becoming opaque and golden in color when illuminated by ultraviolet light (wavelength of 253.7 nm) (*Merzkirch, W. 2007; Quraishi, M. and. Fahidy, T. 1986; Smiths, A.J.and Lim, T.T. 2012; Merzkirch, W. 1987; https://en.wikipedia.org/wiki/Molecular_tagging_velocimetry;https://sr.wikipedia.org/wiki/Supramolecular_hemija; https://en.wikipedia.org/wiki/Quantum_yield).*

Phosphorescent supramolecules solve the biggest problem of photochromic tracers which is low contrast images. This method is based on molecules that will emit light when excited. Essentially, because during the absorption of light there is a change in spin of the electron, so the relaxation also requires a change in spin that will result in the emission of light for a few minutes or hours, in rare cases it can last even a year. The duration of the emission should be long enough for the desired changes in the fluid flow to occur. This method uses a laser to excite molecules, and no light source is needed for imaging. The biggest advantage of using molecular tagging methods if for flow visualization in three dimensions, Figure 4 *(Merzkirch, W. 1987; Smiths, A.J.and Lim, T.T. 2012; Merzkirch, W. 1987; https://en.wikipedia.org/wiki/Quantum_yield; https://sr.wikipedia.org/wiki/Fosforescence; https://sr.wikipedia.org/wiki/Absorption_spectroscopy; https://sh.wikipedia.org/wiki/Paulijev_princip_isklju%C4%8Denja;https://psiberg.com/singlet-vs-triplet-state; https://en.wikipedia.org/wiki/Intersystem; https://en.wikipedia.org/wiki/Forbidden_mechanism).*

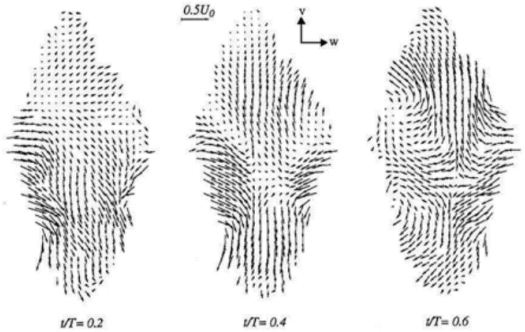

Fig. 4 Vectors direction marked molecule Smiths, A.J.and Lim, T.T. 2012)

The Schlieren method is a modification of shadow photography in terms of optical arrangement and is much more sensitive to changes in density. The level of brightness in the Schlieren method depends on the first derivative of the refractive

index, while in the shadow photography method it depends on the second derivative of the refractive index, i.e. of its Laplacian. In a Schlieren system with parallel light, the parallel light is converged by a lens or spherical mirror called a Schlieren head , and an image of the light source is formed at the focal point of the Schlieren head. At the focus point a knife edge is placed, which is normal to the plane of the test section and will cut off a certain part of the light and thereby reduce the intensity of illumination of the plane on which the photograph is created *Figure 5*. For the Schlieren method, it is mandatory to use a point light source or a light source in the form of a slit, which is then parallel to the edge of the knife (*Quraishi, M. and. Fahidy, T. 1986; Merzkirch, W. 1987; Settles, G.S. 2001; Davidhazy, A. 2006).*

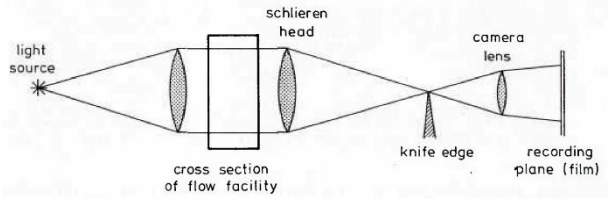

Fig. 5 Topler's Schlieren the system with parallel light (Merzkirch, W. 1987)

There are a certain number of errors introduced by the use of lenses, which affect the quality of the image and thus the precision of the method such as astigmatism and coma. Astigmatism occurs when light rays leaving the lens propagate in two vertical planes that have different focal points, due to astigmatism it is difficult to see fine details in the image. Coma is a phenomenon characterized by the scattering of rays that leave the lens in an area wider than the focus point, it can be caused by irregularities in the lens itself or a light source that is not aligned with the lens, as a result of which objects on the periphery of the photo are no longer seen as points but as elongated cones. These errors can be avoided by using a system where the optical array is shaped as a Latin letter Z and lenses used are parabolic lenses, Figure 6.

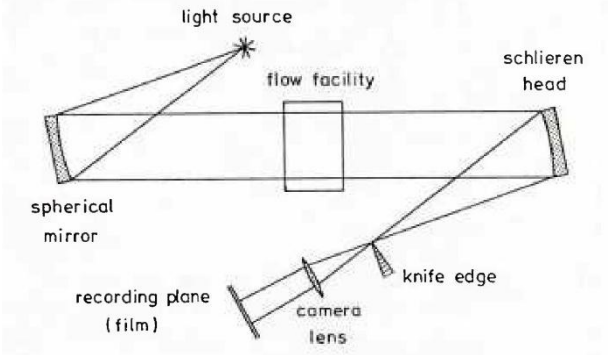

Fig. 6. Z configuration Schlieren's system with parabolic lenses (Merzkirch, W. 1987)

A variation of the method used to increase sensitivity to small changes in density uses a two-pass Schlieren system. Here a conical light source is used and the beam is split by a optical beam splitter. One beam will go by through the exam section two times before coming across the optical beam splitter again, Figure 7. By using this design, astigmatism and coma are almost completely eliminated.

With the help of the Schlieren method, it is possible to obtain color images. This is achieved by using white light as a source and filters located at the focal point of the schlieren head *(Quraishi, M. and. Fahidy, T. 1986; Merzkirch, W. 1987; Settles, G.S. 2001; Davidhazy, A. 2006).*

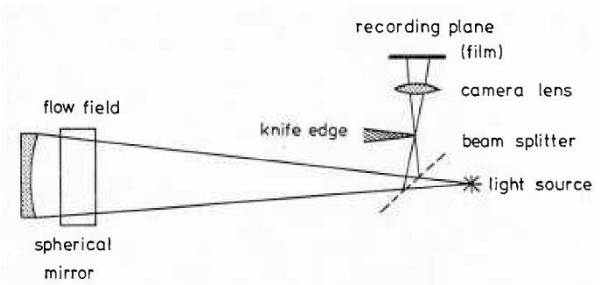

Fig. 7. Two-pass Schlieren's system with optical beam splitter (Merzkirch, W. 1987)

Interference is a reciprocal process when light waves meet that can amplify or cancel each other and the device used for the superposition of light waves is an interferometer. Interferometric methods are based on the principle of the phase delay of the light wave passing through the fluid stream thus forming an integral projection of the refractive index field of the fluid flow. The interferometer separates the light beam from the source with an optical splitter into two waves that will cross different paths, because one is directed towards the reference plane while the other is directed towards the body in this case the fluid flow. This phase delay is then seen as an alternating dark and light picture with the curves containing information regarding the phenomena which is being observed *(Quraishi, M. and. Fahidy, T. 1986; Merzkirch, W. 1987; https://hr.wikipedia.org/wiki/Interferencija_valova; https://en.wikipedia.org/wiki/Wave_interference; https://en.wikipedia.org/wiki/Interferometry; https://sh.wikipedia.org/wiki/Princip_superpozije).*

Digital interferometry, on the other hand, is method where the phase delay is determined very accurately in a large number of points on the picture, *Figure 8*. This method is a combination of holographic interferometry and computer data processing to determine the interferometric phase directly from a group of images. This method can be used to obtain real-time information showing variations in fluid flow and small disturbances that are common in experimental fluid mechanics. This method is suitable for obtaining images of most stable and unstable fluid flows *(Watt,D.W. and Wes, C.M. 1987)*.

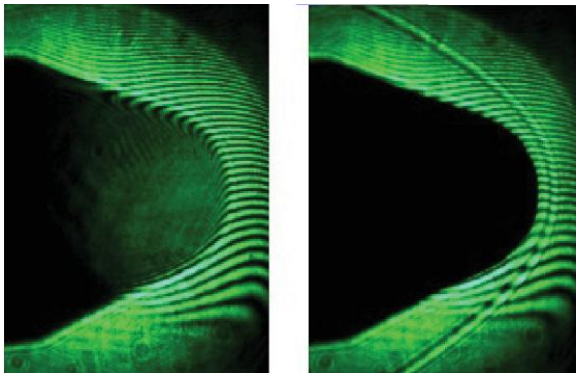

Fig. 8. Digital interferogram of supersonic flow around a blunt object (Tanner, L.H. and Blows, L.G. 1976)

Computational fluid dynamics plays a very important role in fluid mechanics today, due to which it can almost indisputably be viewed as a separate branch of fluid mechanics. The physical properties of fluid flow are dictated by three basic laws, i.e. the law of conservation of mass, the law of conservation of momentum and the law of conservation of energy. These laws are expressed in the form of mathematical equations , which are most often in the form of partial differential equations. CFD deals with the calculation of flow quantities using the Navier-

Stokes equations in order to obtain a complete numerical picture of the analyzed flow. For analyzing complex equation computer visualization is necessary, because human brain has a better understanding visually rather than through the numerical values. Computational fluid dynamics provides the possibility for qualitative verification, checking and verification of models by comparing numerical solutions of CFD models with real life fluid flow . In addition, today CFD is also used for evaluation and optimization of various constructions such cars, airplanes, ports or any other objects that are connected with fluid flow. The development of computational fluid dynamics is closely related to the technological progress of computers and their capacities, so this field is in constant development and progress. Today most CFD software offers graphic options which can visualize the solution the governing equation *(Frits, H. and Walsum, T. 1993; Settles, G.S. 2001; Interferometry-for-High-Speed-Hegde-Jagadeesh; https://cfdflowengineering.com/basics-of-cfd-modeling-for-beginners/#Definition_of_CFD).*

EXPERIMENT

Drag force around the head of a classic axisymmetric projectile model is calculated based on the value of the angle of the oblique shock wave β according to the θ–β–M diagram and according to Schlieren's photo. The drag force is calculated for two initial conditions. The first condition represents the case of projectile being fired from the ground, i.e. under standard conditions (p=101325 Pa; T=288.15 K). The second case represents the firing of a projectile from the average elevation of a fighter plane, where the atmospheric conditions are taken from the table 1 (p =14830 Pa; T =216.7 K). In both cases, the specific gas constant of air is R = 286.9 J/ kgK.

The surface of the head of a classic axisymmetric projectile model is approximated to the surface of the truncated cone with is shown in *Figure 9* and it is calculated in the following way:

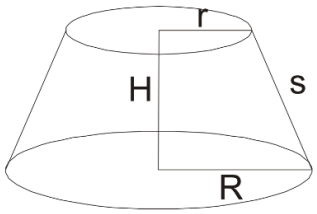

Fig. 9. The appearance of the truncated cone

The envelope derivative of the truncated cone is calculated from the following expression:

$$s = \sqrt{H^2 + (R - r)^2} \quad (1)$$

s – derivative of the envelope of the compartment [m]
H – height of the truncated cone [m]
R, r – radius of the bases of the truncated cone [m]

The area of the hemmed coupe is calculated from the following expression:

$$A = B_1 + B_2 + M = R^2 \cdot \pi + r^2 \cdot \pi + (R + r) \cdot \pi \cdot s \quad (2)$$

A - the surface of the truncated cone
B_1 – surface of the lower base of the truncated cone [m^2]
B_2 – surface of the upper base of the truncated cone [m^2]
M – surface of the roof of the truncated cone [m^2]

To obtain the value of the oblique shock wave angle β_D θ-β-M diagram was used, *Figure 10*. On the abscissa are the values of the angle of the obstacle θ , while on the ordinate are the values of the angle of the oblique shock wave β . The value of the angle of the oblique shock wave is reached by drawing a vertical line from the value of the angle of the obstacle θ to the intersection with the corresponding value of the upstream Mach number, which are represented in the diagram by curved lines, and then by drawing a horizontal line from the intersection point to the ordinate where the value of the angle of the oblique shock wave is read.

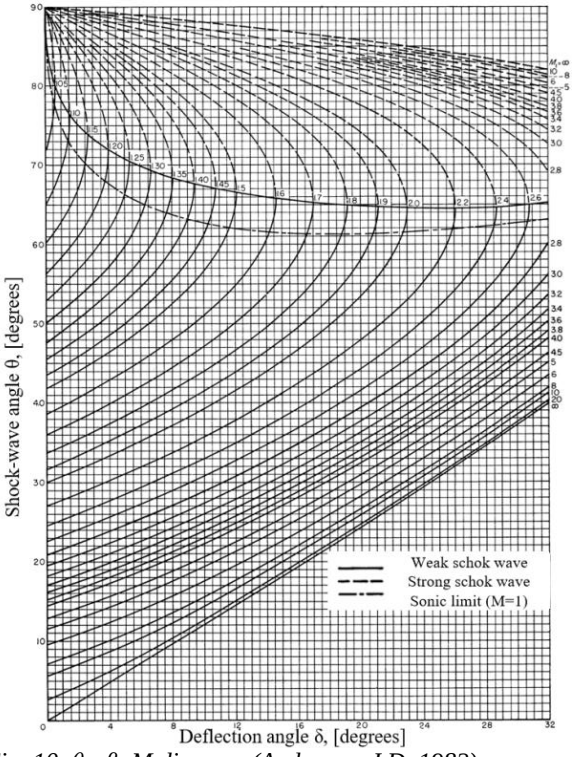

Fig. 10. θ - β -M diagram (Anderson, J.D. 1982)

The second value of the oblique shock wave angle β_S is obtained on the basis of a Schlieren photograph, in Figure 11. The angle β_S was measured from the axis of symmetry of the projectile to the oblique shock wave itself.

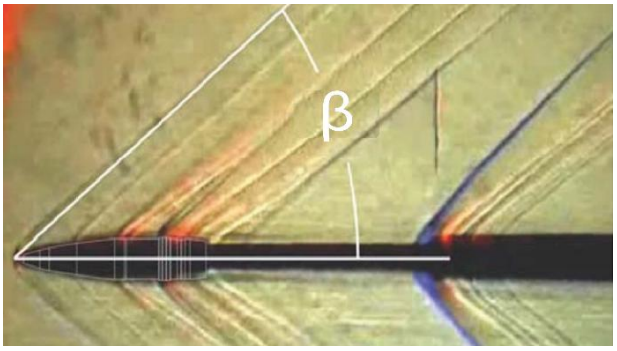

Fig. 11. The angle of the oblique shock wave on the Schlieren photograph

Mach number values are projected onto the direction perpendicular to the oblique shock wave according to the expression:

$$M_{n1}{}^D = M_1 \cdot sin\beta_D \quad (3)$$

$$M_{n1}{}^S = M_1 \cdot sin\beta_S \quad (4)$$

$M_{n1}{}^D$, $M_{n1}{}^S$ - values of the current Mach number projected onto the direction normal to the oblique shock wave [-]
M_1 – value of upstream Mach number parallel to the direction of the axis of symmetry of the projectile [-]
β_D – oblique shock wave angle based on θ-β-M diagram [º]
β_S – the angle of the oblique shock wave based on Schlieren photography [º]

Based on the value of the upstream Mach number projected in the direction perpendicular to the oblique shock wave from the normal shock wave tables (for the isentropes exponent κ =1.4) the ratio of flow parameter values are read.

Table 1. Mach number value for the direction perpendicular to the shock wave

$M_{n1}{}^{D}$	$M_{n2}{}^{D}$	$\frac{p_1}{p_2}$	$\frac{\rho_1}{\rho_2}$	$\frac{T_1}{T_2}$
1.238	0.821	1.627	1.408	1.516

The value of the air density is calculated based on the ideal gas equation :

$$\rho = \frac{p}{R \cdot T} \tag{5}$$

ρ – air density [kg/m^3]
p – air pressure [Pa]
R – specific gas constant of air [J/ kgK]
T – air temperature [K]

The values of the flow parameters after the oblique shock wave are calculated based on flow parameter ratios:

$$p_2 = \frac{p_2}{p_1} \cdot p_1 \tag{6}$$

$$\rho_2 = \frac{\rho_2}{\rho_1} \cdot \rho_1 \tag{7}$$

$$T_2 = \frac{T_2}{T_1} \cdot T_1 \tag{8}$$

p_2 – air pressure after an oblique shock wave [Pa]
ρ_2 – air density after an oblique shock wave [kg/m ^{3}]
T_2 – air temperature after the oblique shock wave [K]
p_1 – air pressure before the oblique shock wave [Pa]
ρ_1 – air density before the oblique shock wave [kg/m ^{3}]
T_1 – air temperature before the oblique shock wave [K]

The drag force is calculated based on the following expression:

$$F_D = \frac{1}{2} \cdot \rho \cdot v^2 \cdot c_D \cdot A \tag{9}$$

where are:
F_D – drag force [N]
ρ – air density [kg/m^3]
v – speed of the body [m/s]
c_D – resistance coefficient [-]
A – body surface [m^2]

While the following expressions were used for calculating the drag force in this paper:

$$F_{D_n} = p_2 \cdot A \tag{10}$$

$$F_D = F_{D_n} \cdot \sin\theta \tag{11}$$

where are:
F_{D_n} – drag force acting in the direction normal to the shock wave [N]
p_2 – air pressure after the oblique shock wave [Pa]
A – body surface [m^2]
F_D – drag force acting in the direction parallel to the axis of symmetry of the projectile [N]
θ – obstacle angle [°]

RESULTS AND DISCUSSION

The results of the value of the drag force around the model of a classical axisymmetric projectile, for three different upstream Mach numbers *(2, 2.5 and 3)* and both initial conditions, based on the value of the angle of the oblique shock wave from the *θ-β-M* diagram and Schlieren photographs are given in *Table 2.*

Table 2. Calculated drag forces for different Mach numbers and initial conditions

			F_D [N]
M=2	p=101325 Pa	β_D	51.76
		β_S	52.98
	p=14830 Pa	β_D	7.57
		β_S	7.75
M=2.5	p=101325 Pa	β_D	55.94
		β_S	54.82
	p=14830 Pa	β_D	8.18
		β_S	8.02
M=3	p=101325 Pa	β_D	61.53
		β_S	63.09
	p=14830 Pa	β_D	8.95
		β_S	8.954

For the analysis the expression (9) will be observed. It is seen that by increasing the Mach number which is dependant on the local fluid flow velocity and the velocity of sound in the given medium will result in an increase of the drag force. On the other hand, with the increase in altitude, there is a drop in pressure, that results in a density drop and therefore a drop in the drag force.

Based on the results of the calculation of the drag force around the model of the classic axisymmetric projectile, it is clear that due to approximations the results deviate significantly from realistic ones. Primarily, an approximation was introduced that only one oblique shock occurs at the front of the projectile, but the actual situation is different. First, a normal shock wave will occur on the projectile's attack point at some distance from it, which becomes a Mach wave far from the axis, passing through all possible states of an oblique shock wave at that distance. Furthermore, this shock wave is followed by a series of oblique shock waves of the same family in accordance with the reduction of the cross-section, until the first expansion waves appear on the point of increase of the cross-section, which are marked in orange-red color in Figure 12 . After that, more oblique shock and expansion waves appear along the projectile. As the pressure through the oblique shock wave increases, and drops through the expansion, it is clear that along the total length of the projectile, the pressure on certain surfaces will differ significantly, complicating the calculation and at the same time affecting the total drag force actin on the projectile. Another important approximation in terms of geometry is that instead of the total surface of the projectile, the calculation was made only for the head of the projectile, which is approximated to a truncated cone. As the projectile in reality has large differences in the diameters of its cross-sections, non-negligible angles at transitions of different diameters and a drastically greater length than the approximated shape, the actual full surface will differ significantly, and as the surface figures in the equation for calculating the drag frorce its values will also differ proportionally. The third approximation refers to the boundary conditions. In the absence of exact values of the boundary conditions during the experiment itself, an approximation was made for two pressure values. One for normal conditions and another for the altitude at which the jet aircraft flies. This approximation does not drastically affect the results themselves because the experiments themselves are set up to simulate real conditions, so with a little research into the purpose of the projectiles they can be estimated with sufficient accuracy.

CONCLUSION

From the selected visualization methods in this paper, their flexibility and ability to adapt to different conditions and

mediums is noticable. For every situation there is a method that will give adequate results. Flow visualization methods have been and still remain an indispensable tool in fluid mechanics, providing researchers with a direct view of fluid phenomena, which is necessary for further research, design, formulating new models, etc. They bridge the gap between theory and practice by providing a deeper and clearer understanding of fluid mechanics.

Nowadays, computational fluid dynamics and conventional methods of fluid flow visualization are narrowly related and complementary in the field of validation, where conventional flow visualization methods serve to compare and improve models in use. In this way the results can be brought closer to realistic conditions, by setting realistic boundary conditions to achieve more accurate results or just to identify regions of interest for study, which can lead to reduction of expenses and time required for simulations. Computational fluid dynamics paired with an adequate visualization method is today the best tool for further research and improvement of engineering practice.

Although the calculation itself is more suitable for the motion of the wedge in supersonic conditions, the main goal of this calculation is to show that Schlieren photography is a valid visualization method for obtaining starting values for a future calculation. The presented methods results are satisfactory, given that the values based on the Schlieren photography and the values based on the diagram or some other calculation method deviate by only a couple of Newtons.

In order to obtain accurate results of the resistance force, one should focus on the analysis of three-dimensional flow (or so-called quasi-two-dimensional flow) over a conical surface *(https://www.engineeringtoolbox.com)*.

REFERENCES

Frits, H.P. and Walsum, T. (1993). Fluid flow visualization, Focus on Scientific Visualization, Springer. pp. 1-40.

W. Merzkirch, Flow visualization, Springer. in 2007

Quraishi,M.S. and Fahidy,T.Z. (1986). Encyclopedia of fluid mechanics 3, University of Waterloo.

Smiths, A.J. and Lim, T.T. (2012). Flow visualization techniques and examples, Imperial College Press.

Merzkirch, W. (1987). Techniques of flow visualization, Advisory Group for Aerospace Research and Development North Atlantic Treaty Organization.

Settles, G.S. (2001). Schlieren and shadowgraph techniques, Springer.

Davidhazy, A. (2006). Introduction to shadowgraph and schlieren imaging, RIT Scholar Works.

Watt, D.W. and West, C.M. (1987). Digital interferometry for flow visualization, Springer-Verlag.

Anderson, J.D. (1982). Modern Compressible Flow, McGraw-Hill Book Company, 1982

Liu, C.Y. and Ng, K.L. (1990). A low-cost mini smoke tunnel with automatic smoke wire fueling mechanism, Int. J. Mec.h. Eng. Educ.

Tanner, L.H. and Blows, L.G. (1976). A study of the motion of oil films on surface in air flow, with application to the measurement of skin friction, J. Phys. E: Sci.

Wikipedia (accessed on 07.05.2023.). https://en.wikipedia.org/wiki/Velocimetry.

Wikipedia (accessed on 07.05.2023.). https://en.wikipedia.org/wiki/Molecular_tagging_velocimetry Wikipedia (accessed on 10.05.2023.). https://sr.wikipedia.org/wiki/Supramolecular_hemija

Wikipedia (accessed on 10.07.2023.). https://en.wikipedia.org/wiki/Quantum_yield

Wikipedia (accessed on 10.07.2023.). https://sr.wikipedia.org/wiki/Fosforescence

Wikipedia (accessed on 17.07.2023.). https://sr.wikipedia.org/wiki/Absorption_spectroscopy

Wikipedia (accessed on 10.07.2023.). https://sh.wikipedia.org/wiki/Paulijev_princip_isklju%C4%8Denja

Wikipedia (accessed on 10.07.2023.). https://en.wikipedia.org/wiki/Intersystem_crossing#:~:text=In%20a%20triplet%20state%20 the,when%20the%20molecule%20absorbs%20radiation.

Wikipedia (accessed on 07.10.2023.). https://en.wikipedia.org/wiki/Forbidden_mechanism

Wikipedia (accessed on 23.07.2023.). https://hr.wikipedia.org/wiki/Interferencija_valova

Wikipedia (accessed on 23.07.2023.). https://en.wikipedia.org/wiki/Wave_interference

Wikipedia (accessed on 23.07.2023.). https://en.wikipedia.org/wiki/Interferometry 23.07.2023

Wikipedia (accessed on 23.07.2023.). https://sh.wikipedia.org/wiki/Princip_superpozije 23.07.2023.

Semantic Scholar (accessed on 23.07.2023.). https://www.semanticscholar.org/paper/Time-Resolved-Digital-Interferometry-for-High-Speed-Hegde-Jagadeesh/76277599fe7266bce9692a342df2b373cd9165e2

CFD Flow Engineering (accessed on 27.07.2023.). https://cfdflowengineering.com/basics-of-cfd-modeling-for-beginners/#Definition_of_CFD

The Engeering ToolBox (accessed on 09.05.2023.). https://www.engineeringtoolbox.com/international-standard-atmosphere-d_985.html 09/05/2023

PsiBerg (accessed on 10.07.2023.). https://psiberg.com/singlet-vs-triplet-state/

Received: 26. 02. 2024. Accepted: 04. 04. 2024.